Arthritis Research & Therapy

RESEARCH ARTICLE Open Access

Total metabolic lesion volume of lymph nodes measured by ^{18}F-FDG PET/CT: a new predictor of macrophage activation syndrome in adult-onset Still's disease

Liyan Wan[1†], Yuting Gao[2†], Jieyu Gu[1], Huihui Chi[1], Zhihong Wang[1], Qiongyi Hu[1], Jinchao Jia[1], Tingting Liu[1], Biao Li[2], Jialin Teng[1], Honglei Liu[1], Xiaobing Cheng[1], Junna Ye[1], Yutong Su[1], Chengde Yang[1*], Hui Shi[1*] and Min Zhang[2*]

Abstract

Background: To investigate the potential utility of quantitative parameters obtained by ^{18}F-fluorodeoxyglucose positron emission tomography/computed tomography (^{18}F-FDG PET/CT) in the assessment of disease severity and the occurrence of macrophage activation syndrome (MAS) in adult-onset Still's disease (AOSD).

Methods: Fifty-seven patients with AOSD who underwent pre-treatment ^{18}F-FDG PET/CT were recruited in this study and compared with 60 age- and sex-matched healthy controls. Clinical features and laboratory data were recorded. The systemic score was assessed to determine the disease severity. The maximal standardized uptake value (SUV_{max}), metabolic lesion volume (MLV), and total lesion glycolysis (TLG) were used to evaluate the involved organs and tissues that abnormally accumulated ^{18}F-FDG. Multivariate analysis was performed to identify the PET/CT-derived risk factors contributing to the AOSD-related MAS, and their diagnostic efficiency was evaluated.

Results: High ^{18}F-FDG accumulation was observed in the bone marrow (SUV_{max} median, 5.10), spleen (SUV_{max} median, 3.70), and lymph nodes (LNs, SUV_{max} median, 5.55). The SUV_{max} of the bone marrow (rho = 0.376, p = 0.004), SUV_{max} of the spleen (rho = 0.450, $p < 0.001$), TLG_{total} of LNs (rho = 0.386, $p = 0.017$), and MLV_{total} of LNs (rho = 0.391, $p = 0.015$) were correlated with the systemic score. The SUV_{max} of the spleen ($p = 0.017$), TLG_{total} of LNs ($p = 0.045$), and MLV_{total} of LNs ($p = 0.012$) were higher in patients with MAS than in those without MAS. A MLV_{total} of LNs > 62.2 (OR 27.375, $p = 0.042$) was an independent predictive factor for MAS with a sensitivity of 80.0% and a specificity of 93.9%.

Conclusions: The glucose metabolic level of the spleen could be an effective and easy-to-use imaging indicator of disease severity, and MLV_{total} of LNs > 62.2 was a strong predictor of MAS occurrence in patients with AOSD.

Keywords: Adult-onset Still's disease, Positron emission tomography/computed tomography, Disease severity, Macrophage activation syndrome

* Correspondence: zm11518@rjh.com.cn; shihui_sjtu@sina.com; yangchengde@sina.com
†Liyan Wan and Yuting Gao are joint first authors.
[1]Department of Rheumatology and Immunology, Ruijin Hospital, Shanghai Jiao Tong University School of Medicine, Shanghai 200025, China
Full list of author information is available at the end of the article

Introduction

Adult-onset Still's disease (AOSD) is a systemic inflammatory disease characterized by spiking fever, salmon-pink evanescent rash, arthralgia, and hepatosplenomegaly [1]. The laboratory profile of AOSD is a reflection of systemic inflammation, including increased erythrocyte sedimentation rate (ESR) and C-reactive protein (CRP), as well as hyperferritinemia, leukocytosis, and elevated levels of cytokines [2]. Diagnosis of AOSD is based on clinical pattern recognition and exclusion of other autoimmune, inflammatory, infectious, or neoplastic diseases [3–5]. The patients with AOSD may experience life-threatening complications, especially companied with macrophage activation syndrome (MAS), with high mortality rate ranging from 10 to 42.5% [6, 7]. Early recognition and treatment of MAS is crucial but challenging, due to the lack of specific markers [8, 9].

^{18}F-fluorodesoxyglucose positron emission tomography/computed tomography (^{18}F-FDG PET/CT), which reflects both the glucose metabolic activity and the anatomical structure of target tissues, is commonly used on cancer diagnosis, staging, and prognosis, assessment of treatment response [10]. For AOSD, ^{18}F-FDG PET/CT has been used as a whole-body imaging tool to exclude malignancies and identify the biopsy sites when the patients were at admission [11, 12]. Previous studies (13 cases [13], seven cases [14], and 26 cases [12]) have revealed the significant increase of FDG uptake of involved organs in patients with AOSD. However, the correlations between abnormal glucose metabolism of involved organs, as determined by the maximal standardized uptake value (SUV_{max}), and disease severity are still illusive.

PET/CT-derived quantitative parameters based on three-dimensional volume of interest (VOI), namely metabolic tumor volume (MTV) and total lesion glycolysis (TLG), have been widely used in the assessment of whole-body disease burden and prognosis of tumors [15, 16]. Interestingly, recent studies presented associations between TLG and systemic inflammation in patients with recurrent colorectal cancer [17] and IgG_4-related disease [18]. Here, we quantified ^{18}F-FDG uptake in patients with AOSD using SUV, MTV, and TLG, in pursuit of identifying markers associated with disease severity and AOSD-related MAS as well.

Material and methods

Patient recruitment

From November 2015 to January 2019, we identified 57 hospitalized patients diagnosed with AOSD according to the classification criteria proposed by Yamaguchi et al. at an academic hospital [4]. Clinical manifestations and laboratory data were obtained on admission, and a systemic score, as proposed by Pouchot [19], was assessed for each patient. Macrophage activation syndrome (MAS) was diagnosed based on HLH-2004 criteria [20]. All patients underwent ^{18}F-FDG PET/CT scan for excluding malignancy before treatments of AOSD. In addition, to determine the glucose metabolic level of normal tissues and organs on PET/CT, 60 age- and sex-matched healthy controls without a history of autoimmune disease, recent infection, or malignant tumor were retrospectively recruited. The study was approved by the Ethics Committee of Ruijin Hospital, Shanghai Jiao Tong University School of Medicine.

PET/CT scanning

^{18}F-FDG PET/CT scanning was performed using the Discovery VCT64 system (GE Healthcare, Chicago, IL, USA). To control the blood glucose concentration below 7.4 mmol/L before scanning, patients were instructed to fast for at least 6 h. Patients received an intravenous injection of 5–6 MBq of ^{18}F-FDG per kilogram of body weight 45–60 min before scanning from the skull base to the mid-thigh. PET images were acquired for 3 min per bed position using a matrix size of 128 × 128, 28 subsets, two iterations, and full-width half-maximum post-filtering. CT images were acquired using a tube voltage of 140 kV, a tube current of 220 mA, and a section thickness of 3.75 mm. The reconstruction of PET images was based on an ordered-subset expectation maximization algorithm with photon attenuation correction using CT data.

PET/CT image interpretation

Integrated PET and CT images were independently interpreted by two nuclear medicine physicians on the Advantage Workstation 4.4 system (GE Healthcare). The glucose metabolic level of the bone marrow, spleen, liver, and lymph nodes (LNs) in all patients with AOSD were assessed by the SUV_{max} and SUV_{mean} within the VOI drawn on the PET/CT images. The abnormal hypermetabolism of these organs and tissues were defined as SUV_{max} higher than the upper limit of the 95% confidence interval for the glucose metabolic level of them in the healthy controls. LNs with ^{18}F-FDG uptake lower than blood pool were excluded from analyses. In this study, the MTV was renamed as the metabolic lesion volume (MLV) because AOSD-affected lesions were non-neoplastic. Both the MLV and TLG [18] were measured on all hypermetabolic LNs. The MLV was automatically delineated using a threshold of 40% of the SUV_{max}. The TLG was defined as the MLV multiplied by the SUV_{mean}. The total MLV (MLV_{total}), which summed MTVs, and the total TLG (TLG_{total}), which summed TLGs, in all hypermetabolic LNs were measured as the quantitative parameters of whole-body disease burden. Because of the irregular shape of the bone marrow and spleen, and the vicinity of the physiologically ^{18}F-FDG-avid kidney, it was difficult to obtain VOIs

completely covering either organ where the MLV and TLG could not be measured.

Statistical analysis

Statistical analysis was performed using SPSS (version 23, IBM Corporation) and R (version 3.6.2) software packages. Chi-square and Fisher's exact tests were used to compare categorical variables. The Mann-Whitney rank sum test was used to compare continuous variables with non-normal distribution after the Kolmogorov-Smirnov test. The Wilcoxon signed-rank test was used to compare paired continuous variables with non-normal distribution. Spearman's correlations were analyzed to examine the relationship between PET/CT parameters and laboratory indices with a Bonferroni correction. Binary logistic regression and Firth logistic regression [21] were used to evaluate the contribution of different clinical risk factors to disease severity. All the variables were included in the regression mode. The variables with $p < 0.1$ in univariate analysis were entered in multivariate analysis. Multicollinearity was excluded from the final model. Receiver operating characteristic curves (ROCs) were performed to determine the diagnostic performance of the PET/CT parameters. The optimum cutoff value was defined based on the maximum Youden index. The diagnostic accuracy of each parameter was reported together with its 95% confidence interval (CI). Statistical significance was defined as $p < 0.05$.

Results

Clinical information of patients with AOSD

All the information is presented in Table 1. The median age of the 57 patients was 34, with a female predominance of 84.21%. The most prevalent clinical manifestations were arthralgia (91.23%) and skin rash (91.23%), followed by fever higher than 39 °C (80.70%). Increased levels of CRP (94.74%), serum ferritin (87.72%), and ESR (73.68%) were commonly observed. The median systemic score was 7.

Table 1 Patient characteristics

Demographics	
Number	57
Age (y)	34 (26–47)
Female	48/9
Disease duration (months)	3 (1–12)
Clinical features	
Fever > 39 °C	46 (80.7)
Skin rash	52 (91.2)
Arthralgia	52 (91.2)
Sore throat	44 (77.2)
Lymphadenopathy	43 (75.4)
Splenomegaly	25 (43.9)
Hepatomegaly	9 (15.8)
Pleuritis	20 (35.1)
Pericarditis	14 (24.6)
Weight loss	14 (24.6)
Lung disease	1 (1.8)
Laboratory findings	
Leukocytosis (> 10,000/mm^3)	34 (59.7)
Neutrophils (> 80%)	36 (63.2)
Hb < 90 g/L	9 (15.8)
PLT < 100,000/mm^3	2 (3.5)
ESR > 40 mm/h	42 (73.7)
CRP > ULN	54 (94.7)
Serum ferritin > 5 ULN	36 (63.2)
Abnormal liver function	36 (63.2)
Negative ANA (titer ≤ 1:80)	54 (94.7)
Negative RF	56 (98.2)
IL2R > ULN	33/45 (73.3)
Pouchot score	7 (5–7.5)

Data are presented in the form of median (Q1–Q3) as continuous variable or as absolute number (percentage of the total patients%);
ULN upper limit of normal, *Hb* hemoglobin, *PLT* platelet, *ESR* erythrocyte sedimentation rate, *ANA* antinuclear antibody, *RF* rheumatoid factor, *CRP* C-reactive protein, *IL-2R* interleukin-2 receptor

Characterization of abnormal ^{18}F-FDG accumulation in patients with AOSD

The accumulation of ^{18}F-FDG was significantly higher in the bone marrow, spleen, and LNs in patients with AOSD than healthy controls, except for ^{18}F-FDG uptake in the liver ($p = 0.672$) (Table 2). Representative PET/CT images of abnormal hypermetabolic distributions in two patients with AOSD are depicted in Fig. 1.

Bone marrow hypermetabolism occurred in 61.40% (35/57) of the patients, while spleen hypermetabolism occurred in 75.44% (43/57) of the patients. 66.7% (38/57) patients showed hypermetabolic LNs. In these cases, bilateral distribution of hypermetabolic LNs was commonly observed. The most commonly involved superficial LNs were cervical LNs (30/38, 78.95%) and axillary LNs (27/38, 71.05%), followed by inguinal LNs (13/38, 34.21%). Deep hypermetabolic LNs were also frequently observed, ranking with mediastinum LNs (19/38, 50.00%), pelvic LNs (16/38, 42.11%), retroperitoneal LNs (14/38, 36.84%), and abdominal LNs (8/38, 21.05%). In addition, four patients exhibited hypermetabolic LNs at the unilateral upper arm (intra-muscle).

Because of the limited scan range of PET/CT in this study, only the hip and shoulder joints were evaluated. Increased ^{18}F-FDG uptake by the hip joints was only seen in one patient, with a SUV_{max} of 3.1, whereas three patients showed hypermetabolic shoulder joints with SUV_{max} of 3.1–3.3.

Table 2 ^{18}F-FDG accumulation in the mainly involved organs and tissues in patients with AOSD compared with healthy controls

	N (%)	SUV_{max} in patients with AOSD	Bilateral (*n*)	SUV_{max} in healthy controls	*p*
Bone marrow	–	5.10 (4.25–6.10)	–	3.76 (3.00–4.15)	< 0.001
Spleen	–	3.70 (3.05–4.35)	–	2.28 (2.06–2.56)	< 0.001
Liver	–	3.20 (2.80–3.60)	–	3.26 (2.88–3.58)	0.672
Lymph nodes[#]	38 (66.67)	5.55 (4.05–8.68)	–	–	–
Cervical LN	30 (52.63)	5.15 (3.92–7.85)	26/30	–	–
Axillary LN	27 (47.37)	4.70 (2.70–6.00)	25/27	–	–
Mediastinum LN	19 (33.33)	5.30 (3.70–8.90)	–	–	–
Pelvic LN	16 (28.07)	6.45 (4.68–8.52)	–	–	–
Retroperitoneal LN	14 (24.56)	5.60 (3.15–7.72)	–	–	–
Inguinal LN	13 (22.81)	4.20 (2.65–5.20)	10/13	–	–
Abdominal LN	8 (14.04)	6.60 (5.25–7.70)	–	–	–

Data are presented in the form of median (Q1–Q3) as continuous variable
SUV standardized uptake value
[#]This was calculated from the patients with hypermetabolic lymph nodes ($n = 38$). SUVmax was the maximum SUV of the regional lymph node

Abnormal FDG uptake by the right subscapularis was observed in only one patient. There was no increased ^{18}F-FDG uptake by the skin in our cohort. In addition, there was only one (1.75%) patient in our cohort who showed parenchymal lung involvement with a SUV_{max} of 2.2 on the lung.

Correlations between laboratory findings, systemic score, and PET/CT parameters

The correlations between disease severity-related laboratory findings and PET/CT parameters are summarized in Table S1. The spleen hypermetabolism showed positive correlations with ferritin (rho = 0.478, $p < 0.001$),

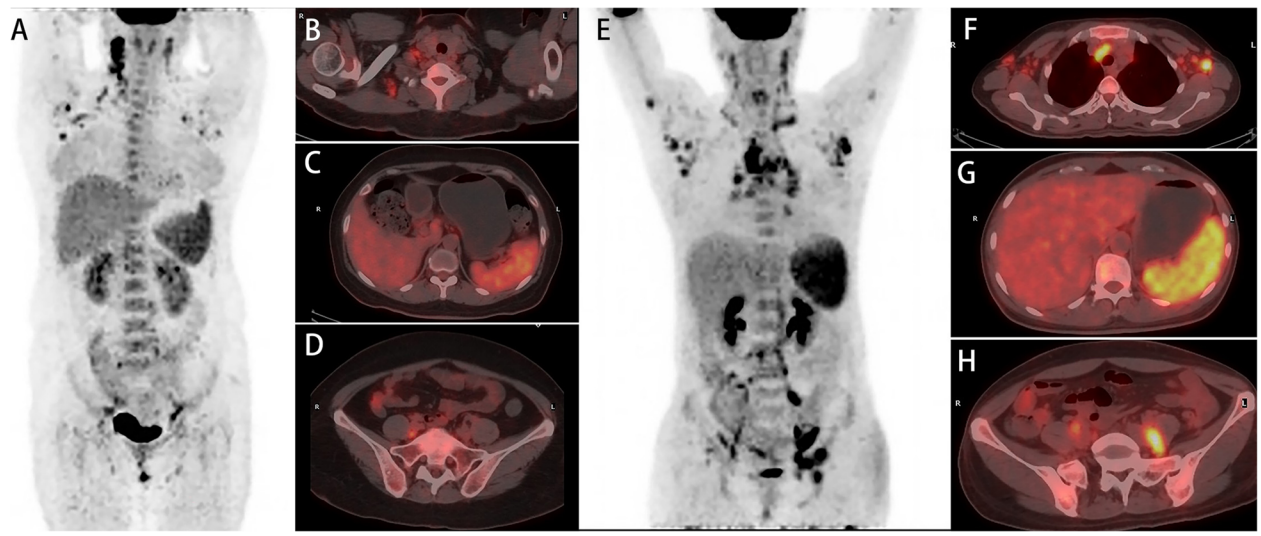

Fig. 1 Whole-body PET image (**a**) and axial hybrid PET/CT images of the axillary LNs (**b**), liver and spleen (**c**), and pelvis bone (**d**) from a 45-year-old female patient with fever, skin rash, and arthralgia showed increased ^{18}F-FDG uptake by the right axillary LNs (SUV_{max}, 6.7), spleen (SUV_{max}, 4.7), liver (SUV_{max}, 3.3), and pelvic bone marrow (SUV_{max}, 4.3). The TLG_{total} of LNs was 199,697.4, and MLV_{total} of LNs was 53.88. The patient did not progress to MAS after glucocorticoids and methotrexate treatment. Another 42-year-old female patient with fever, skin rash, and lymphadenopathy showed increased ^{18}F-FDG uptake by the left axillary LNs (SUV_{max}, 9.8), mediastinum LNs (SUV_{max}, 11.4), spleen (SUV_{max}, 7.5), liver (SUV_{max}, 4.7), and pelvic bone marrow (SUV_{max}, 5.1) on whole-body PET image (**e**) and axial hybrid PET/CT images of the axillary and mediastinum LNs (**f**), liver and spleen (**g**), and pelvis bone (**h**). The TLG_{total} of LNs was 1,144,469.8, and MLV_{total} of LNs was 244.75. The patient progressed to MAS after glucocorticoid treatment. Lately, she received intravenous immunoglobulins and achieved remission. LNs, lymph nodes; SUV, standardized uptake value; TLG, total lesion glycolysis; MLV, metabolic lesion volume; MAS, macrophage activation syndrome

lactate dehydrogenase (LDH) (rho = 0.462, $p < 0.001$), and interleukin-2 receptor (IL-2R) (rho = 0.454, $p = 0.002$). The SUV_{max} of the LN negatively correlated with the white blood cell count (rho = − 0.500, $p = 0.001$). The MLV_{total} of LNs displayed a positive correlation with the levels of IL-2R (rho = 0.495, $p = 0.004$).

The systemic score is a widely used indicator of AOSD disease severity. The SUV_{max} of the spleen (rho = 0.450, $p < 0.001$), SUV_{max} of the bone marrow (rho = 0.376, $p = 0.004$), TLG_{total} (rho = 0.386, $p = 0.017$), and MLV_{total} (rho = 0.391, $p = 0.015$) of LNs showed significant correlations with the systemic score (Fig. 2). Notably, the patients with systemic score ≥ 7 showed significantly higher SUV_{max} of the bone marrow ($p = 0.005$), spleen ($p = 0.002$), TLG_{total} ($p = 0.044$), and MLV_{total} ($p = 0.033$) of LNs than those with systemic score < 7 (Table S2).

PET/CT features in MAS

Eight of 57 patients were diagnosed with MAS during the current hospitalization and underwent PET/CT scanning before the diagnosis of MAS. The time interval between PET/CT scanning and the diagnosis of MAS ranged from 2 to 33 days (Table S3). Only two patients showed cytopenia involving cells of 1 lineage, suggesting MAS might be in development when performing PET/CT.

Patients with MAS showed significantly higher SUV_{max} of the spleen ($p = 0.017$, $n = 8$), TLG_{total} ($p = 0.045$, $n = 5$), and MLV_{total} of LNs ($p = 0.012$, $n = 5$) compared to patients without MAS (Table 3). Considering the high mortality rate of MAS, the risk factors for MAS were assessed (Table 4). ROC analyses revealed that MLV_{total} of LNs > 62.2, SUV_{max} of the spleen > 3.55, and TLG_{total} of LNs > 248,040 were the optimal cut-points for discriminating MAS occurrence. Elevated levels of LDH, IL-2R, platelet count, TLG_{total} of LNs > 248,040, SUV_{max} of the spleen > 3.55, and MLV_{total} of LNs > 62.2 significantly associated with MAS occurrence in univariate analysis. Subsequent multivariate analyses indicated that elevated IL-2R level and MLV_{total} of LNs > 62.2 were independent risk factors of MAS.

MLV_{total} of LNs > 62.2 had a sensitivity of 80.0%, a specificity of 93.9%, and an AUC of 0.855 in predicting MAS occurrence, which were comparable with those of the traditional marker, IL-2R (sensitivity, 75.0%; specificity, 97.3%; AUC, 0.899). Level of ferritin, SUV_{max} of the spleen, and the systemic score showed low specificity of 40.8–55.1% and AUC of 0.642–0.765 (Table 5).

Discussion

^{18}F-FDG PET/CT is a useful tool to rule out malignancy before the diagnosis of AOSD. The additional values including the potential correlations between the PET/CT findings and disease assessments are worth to be investigated. Hypermetabolic status of the bone marrow, spleen, and LNs in patients with AOSD have been observed in other studies [11–14, 22–25]. We further explored the utility of PET/CT to assess disease severity and MAS occurrence of AOSD. Our study suggests that PET/CT could act as an early detective tool to evaluate the disease severity and predict the occurrence of deadly complication, MAS, in patients with AOSD.

The glucose metabolic level of the spleen could be an effective indicator of AOSD severity. In the present study, not only positive correlations between SUV_{max} of

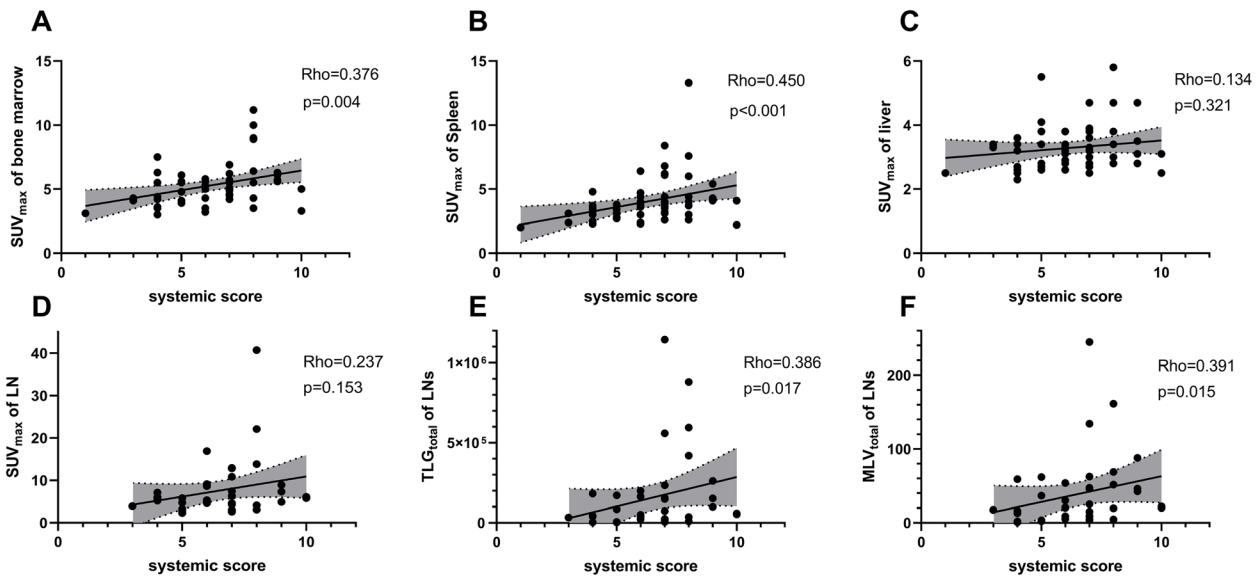

Fig. 2 Correlations between the SUV_{max} of the bone marrow (**a**), spleen (**b**), liver (**c**), LNs (**d**), TLG_{total} (**e**), MLV_{total}, (**f**) of LNs, and the systemic score. SUV, standardized uptake value; TLG, total lesion glycolysis; MLV, metabolic lesion volume. Significance was set at $p < 0.05$

Table 3 Comparison of PET/CT parameters between the patients with and without MAS

	Patients with MAS	Patients without MAS	*p*
	n = 8	*n* = 49	
SUV_{max} of the bone marrow	4.95 (3.68–5.40)	5.50 (4.30–6.15)	0.214
SUV_{max} of the spleen	4.35 (3.78–5.75)	3.50 (3.00–4.10)	0.017
SUV_{max} of the liver	3.10 (2.85–3.65)	3.30 (2.75–3.60)	0.854
SUV_{max} of LNs	7.30 (4.65–11.80)	5.20 (4.00–8.00)	0.271
TLG_{total} of LNs	261,170.20 (86,548.35–851,990.60)	44,518.30 (8828.20–159,463.70)	0.045
MLV_{total} of LNs	87.81 (38.78–189.47)	20.05 (4.74–46.12)	0.012

Data are presented in the form of median (Q1–Q3) as continuous variable

the spleen and those laboratory profiles of AOSD including the levels of LDH, ferritin, and IL-2R were observed, but also the hypermetabolism of the spleen showed a higher correlation coefficient with systemic score and more frequent occurrence in patients with AOSD than those of the bone marrow and LNs. We assumed that the enhanced FDG accumulation in the spleen may be secondary to inflammation and hypercytokinemia [26]. Furthermore, compared to the bone marrow and LNs, the spleen as a morphologically oblate and single organ is more likely to be drawn in a VOI on PET/CT images for more reliably and easily measuring its glucose metabolic levels in clinical practice. Additionally, a negative correlation between SUV_{max} of LNs and the white blood cell count was observed, which might be due to virus infection which was known as a trigger to AOSD [27–29], thereby temporarily disrupting the homeostasis of the bone marrow [30]. Although both elevated [24] and reduced [31] ^{18}F-FDG uptake of the liver was observed in previous case reports, there was no statistical difference of SUV_{max} of the liver between patients with AOSD and healthy controls in our study. Similar to the studies of Dong et al. [12] and Jiang et al. [11], the prevalence of articular involvement in our cohort (10.53%) was low, indicating that increased ^{18}F-FDG uptake in the joints may not be significant in patients with AOSD, which was probably due to the relatively mild involvement of joints in Chinese patients [32].

MLV_{total} of LNs was a promising useful predictor of MAS occurrence in patients with AOSD. Previous studies have reported that ^{18}F-FDG PET/CT-derived quantitative parameters were associated with the occurrence [33] or outcome of MAS [34, 35]. In our study, we further found that MLV_{total} of LNs had better diagnostic performance than SUV_{max} of the spleen and TLG_{total} of LNs for distinguishing patients with MAS from those without MAS. Hypermetabolism of whole-body LNs is believed to be due to the high accumulation of inflammatory cells and the over-activation of the mononuclear phagocyte system in LNs [34, 36]. Patients with MLV_{total} of LNs > 62.2 showed a 20-fold increased risk for MAS occurrence than those with MLV_{total} of LNs less than or equal to 62.2. IL-2R may serve as a good laboratory indicator of MAS [37]. In this study, the IL-2R level was also an independent factor for predicting MAS occurrence with comparably high likelihood ratios to MLV_{total} of LNs. Even if the predictive value of IL-2R, as a cheaper test than PET/CT, was already high, the value of PET/

Table 4 Risk factors for the occurrence of MAS

	Univariate analysis			Multivariate analysis		
	p	OR	95% CI	*p*	OR	95% CI
Age	0.138	0.955	0.898–1.015			
Sex	0.784	1.366	0.147–12.677			
LDH	0.009	1.005	1.001–1.008			
PLT	0.035	0.992	0.984–0.999			
IL-2R	0.002	1.002	1.001–1.003	0.002	1.003	1.001–1.007
SUV_{max} of the spleen > 3.55	0.004	19.170	2.182–2528.558			
TLG_{total} of LNs > 248,040	0.013	15.000	1.752–128.391			
MLV_{total} of LNs > 62.2	0.002	62.000	4.529–848.704	0.042	27.375	1.117–123,080.200

Both TLG_{total} and MLV_{total} of LNs were calculated from the patients with hypermetabolic lymph nodes ($n = 38$). All laboratory variables were included in logistic regression, and only the results with $p < 0.1$ were listed here

LDH lactate dehydrogenase, *PLT* platelet, *IL-2R* interleukin-2 receptor, *SUV* standardized uptake value, *LN* lymph node, *TLG* total lesion glycolysis, *MLV* metabolic lesion volume, *MAS* macrophage activation syndrome

Table 5 The AUC, sensitivity, specificity, and likelihood ratio of PET/CT parameters, serologic markers, and systemic scoring for predicting the occurrence of MAS

Factor	AUC (95% CI)	Cutoff value	Sensitivity, % (95% CI)	Specificity, % (95% CI)	Likelihood ratio
IL-2R	0.899 (0.776–0.999)	2824 pg/ml	75.0 (40.9–95.6)	97.3 (48.7–99.9)	27.8
MLV_{total} of LNs	0.855 (0.642–0.999)	62.2	80.0 (37.6–99.0)	93.9 (80.4–98.9)	13.2
SUV_{max} of the spleen	0.765 (0.630–0.900)	3.55	100.0 (67.6–100.0)	53.1 (39.4–66.3)	2.13
Systemic score ≥ 7	0.713 (0.541–0.885)		87.5 (52.9–99.4)	55.1 (41.3–68.1)	1.95
Ferritin > 5 ULN	0.642 (0.455–0.828)		87.5 (52.9–99.4)	40.8 (28.2–54.8)	1.48

LN lymph node, *MLV* metabolic lesion volume, *IL-2R* interleukin-2 receptor, *MAS* macrophage activation syndrome. MLV_{total} of LNs were calculated from the patients with hypermetabolic lymph nodes ($n = 38$)

CT was not negligible. Firstly, the performance of IL-2R for diagnosing MAS is still limited [38, 39], especially with low specificity (38.8–72.5%). Secondly, PET/CT has been routinely used to rule out malignancy in the diagnosis of AOSD. Its evaluation of the MAS occurrence could bring additional diagnostic information to clinicians. We believe that the combined diagnosis of IL-2R and MLV_{total} of LNs may have better predictive performance for MAS, but this conclusion cannot be obtained due to the limited number of samples in the present study. Therefore, further attention should be given to the whole-body inflammatory burden reflected by the MLV_{total} of LNs for assessing the risk of MAS in patients with AOSD. Recently, the negative prognostic impact of lung involvement in patients with AOSD has been reported [40], and the lung involvement has been correlated with the occurrence of MAS [41, 42]. However, due to the low prevalence of parenchymal lung involvement in our study, no inferential analysis was made.

There are still some limitations in this study. (a) The number of cases with MAS was low ($n = 8$) leading to the possibility of model overfitting. (b) Short-term glucocorticoid treatment before PET/CT scanning in some patients may have a limited effect on the accuracy of SUV measurement [43]. (c) There was a short time interval between PET/CT and diagnosis of MAS in two patients, whereas other six patients were diagnosed with MAS 1 week after PET/CT scan. Therefore, PET/CT may act as an actual display of the current disease activity as well as a prediction over time. This study was a pilot study at a single center, and more high evidence studies are needed to verify the reliability of the PET/CT parameters in the assessment of disease severity and the prediction of MAS in patients with AOSD.

Conclusions

Our data revealed that the glucose metabolic level of the spleen could be an effective and easy-to-use imaging indicator of disease severity, and MLV_{total} of LNs > 62.2 was a strong predictor of MAS occurrence in patients with AOSD.

Abbreviations

^{18}F-FDG PET/CT: ^{18}F-fluorodeoxyglucose positron emission tomography/computed tomography; AOSD: Adult-onset Still's disease; AUC: Area under the curve; CI: Confidence interval; CRP: C-reactive protein; csDMARDs: Conventional synthetic disease-modifying anti-rheumatic drugs; CT: Computer tomography; ESR: Erythrocyte sedimentation rate; IL: Interleukin; LNs: Lymph nodes; MAS: Macrophage activation syndrome; MLV_{total}: Total metabolic lesion volume; MRI: Magnetic resonance imaging; VOI: Volume of interest; MTX: Methotrexate; NSAIDs: Nonsteroidal anti-inflammatory drugs; SUV_{max}: Maximal standardized uptake value; MTV: Metabolic tumor volume; TLG: Total lesion glycolysis; TNF: Tumor necrosis factor; TLG_{total}: Total lesion glycolysis; ROC: Receiver operating characteristic curve

Supplementary Information

Supplementary information accompanies this paper at https://doi.org/10.1186/s13075-021-02482-2.

Additional file 1: Table S1. Correlations between disease severity-related laboratory findings, systemic score, and PET/CT parameters. **Table S2.** Comparison of PET/CT parameters between patients with systemic score ≥ 7 and patients with systemic score <7. **Table S3.** Characteristic of eight patients with MAS.

Authors' contributions

MZ, HS, and CD Y designed the project and supervised the project. HH C, ZH W, QY H, CD Y, H S, JC J, LY W, and JY G collected the clinical data. MZ and YT G read the scans. LY W and JY G analyzed the data and performed statistical analyses. LY W, JY G, and TT L wrote the manuscript with contributions from all authors. The authors read and approved the final manuscript.

Funding

This work was supported by grants from Shanghai Jiao Tong University Medicine and Engineering Interdisciplinary Funding (YG2017MS61, YG2017QN58, and ZH2018QNA47), Shanghai Municipal Key Clinical Specialty (shslczdzk03403), and Shanghai Pujiang Program (18PJD030).

Availability of data and materials

All data generated or analyzed during this study are included in this published article and its supplementary information files.

Declarations

Ethics approval and consent to participate

The study was approved by the Ethics Committee of Ruijin Hospital, Shanghai Jiao Tong University School of Medicine. As a retrospective study, this study was exempt from informed consent.

Consent for publication

Not applicable.

Competing interests

The authors declare that they have no competing interests.

Author details

[1]Department of Rheumatology and Immunology, Ruijin Hospital, Shanghai Jiao Tong University School of Medicine, Shanghai 200025, China. [2]Department of Nuclear Medicine, Ruijin Hospital, Shanghai Jiao Tong University School of Medicine, 197 Ruijin 2nd Road, Shanghai 200025, China.

Received: 7 November 2020 Accepted: 17 March 2021
Published online: 30 March 2021

References

1. Giacomelli R, Ruscitti P, Shoenfeld Y. A comprehensive review on adult onset Still's disease. J Autoimmun. 2018;93:24–36. https://doi.org/10.1016/j.jaut.2018.07.018.
2. Jamilloux Y, Gerfaud-Valentin M, Martinon F, Belot A, Henry T, Sève P. Pathogenesis of adult-onset Still's disease: new insights from the juvenile counterpart. Immunol Res. 2015;61(1–2):53–62. https://doi.org/10.1007/s12026-014-8561-9.
3. Cush JJ, Medsger TA, Christy WC, Herbert DC, Cooperstein LA. Adult-onset Still's disease. Clinical course and outcome. Arthritis Rheum. 1987;30(2):186–94. https://doi.org/10.1002/art.1780300209.
4. Yamaguchi M, Ohta A, Tsunematsu T, Kasukawa R, Mizushima Y, Kashiwagi H, Kashiwazaki S, Tanimoto K, Matsumoto Y, Ota T. Preliminary criteria for classification of adult Still's disease. J Rheumatol. 1992;19(3):424–30.
5. Fautrel B, Zing E, Golmard J-L, Le Moel G, Bissery A, Rioux C, Rozenberg S, Piette J-C, Bourgeois P. Proposal for a new set of classification criteria for adult-onset still disease. Medicine. 2002;81(3):194–200. https://doi.org/10.1097/00005792-200205000-00003.
6. Ruscitti P, Rago C, Breda L, Cipriani P, Liakouli V, Berardicurti O, Carubbi F, Di Battista C, Verrotti A, Giacomelli R. Macrophage activation syndrome in Still's disease: analysis of clinical characteristics and survival in paediatric and adult patients. Clin Rheumatol. 2017;36(12):2839–45. https://doi.org/10.1007/s10067-017-3830-3.
7. Ruscitti P, Cipriani P, Ciccia F, Masedu F, Liakouli V, Carubbi F, Berardicurti O, Guggino G, Di Benedetto P, Di Bartolomeo S, et al. Prognostic factors of macrophage activation syndrome, at the time of diagnosis, in adult patients affected by autoimmune disease: analysis of 41 cases collected in 2 rheumatologic centers. Autoimmun Rev. 2017;16(1):16–21. https://doi.org/10.1016/j.autrev.2016.09.016.
8. Kostik MM, Dubko MF, Masalova VV, Snegireva LS, Kornishina TL, Chikova IA, Likhacheva TS, Isupova EA, Glebova NI, Kuchinskaya EM, Balbotkina EV, Buchinskaya NV, Kalashnikova OV, Chasnyk VG. Identification of the best cutoff points and clinical signs specific for early recognition of macrophage activation syndrome in active systemic juvenile idiopathic arthritis. Semin Arthritis Rheum. 2015;44(4):417–22. https://doi.org/10.1016/j.semarthrit.2014.09.004.
9. Wang R, Li T, Ye S, Tan W, Zhao C, Li Y, de Bao C, Fu Q. Macrophage activation syndrome associated with adult-onset Still's disease: a multicenter retrospective analysis. Clin Rheumatol. 2020;39(8):2379–86. https://doi.org/10.1007/s10067-020-04949-0.
10. Scarsbrook AF, Barrington SF. PET-CT in the UK: current status and future directions. Clin Radiol. 2016;71(7):673–90. https://doi.org/10.1016/j.crad.2016.02.023.
11. Jiang L, Xiu Y, Gu T, Dong C, Wu B, Shi H. Imaging characteristics of adult onset Still's disease demonstrated with 18F-FDG PET/CT. Mol Med Rep. 2017;16(3):3680–6. https://doi.org/10.3892/mmr.2017.7022.
12. Dong MJ, Wang CQ, Zhao K, Wang GL, Sun ML, Liu ZF, Xu L. 18F-FDG PET/CT in patients with adult-onset Still's disease. Clin Rheumatol. 2015;34(12):2047–56. https://doi.org/10.1007/s10067-015-2901-6.
13. An Y-S, Suh C-H, Jung J-Y, Cho H, Kim H-A. The role of 18F-fluorodeoxyglucose positron emission tomography in the assessment of disease activity of adult-onset Still's disease. Korean J Intern Med. 2017;32(6):1082–9. https://doi.org/10.3904/kjim.2015.322.
14. Yamashita H, Kubota K, Takahashi Y, Minamimoto R, Morooka M, Kaneko H, Kano T, Mimori A. Clinical value of ^{18}F-fluoro-dexoxyglucose positron emission tomography/computed tomography in patients with adult-onset Still's disease: a seven-case series and review of the literature. Mod Rheumatol. 2014;24(4):645–50. https://doi.org/10.3109/14397595.2013.850998.
15. Zhang C, Liao C, Penney BC, Appelbaum DE, Simon CA, Pu Y. Relationship between overall survival of patients with non-small cell lung cancer and whole-body metabolic tumor burden seen on postsurgical fluorodeoxyglucose PET images. Radiology. 2015;275(3):862–9. https://doi.org/10.1148/radiol.14141398.
16. Sharma A, Mohan A, Bhalla AS, Sharma MC, Vishnubhatla S, Das CJ, Pandey AK, Sekhar Bal C, Patel CD, Sharma P, Agarwal KK, Kumar R. Role of Various Metabolic Parameters Derived From Baseline 18F-FDG PET/CT as Prognostic Markers in Non-Small Cell Lung Cancer Patients Undergoing Platinum-Based Chemotherapy. Clin Nucl Med. 2018;43(1):e8–e17. https://doi.org/10.1097/RLU.0000000000001886.
17. McSorley ST, Khor BY, Tsang K, Colville D, Han S, Horgan PG, McMillan DC. The relationship between F-FDG-PETCT-derived markers of tumour metabolism and systemic inflammation in patients with recurrent disease following surgery for colorectal cancer. Color Dis. 2018;20(5):407–15. https://doi.org/10.1111/codi.13973.
18. Berti A, Della-Torre E, Gallivanone F, Canevari C, Milani R, Lanzillotta M, Campochiaro C, Ramirez GA, Bozzalla Cassione E, Bozzolo E, et al. Quantitative measurement of 18F-FDG PET/CT uptake reflects the expansion of circulating plasmablasts in IgG4-related disease. Rheumatology (Oxford). 2017;56(12):2084–92.
19. Pouchot J, Sampalis JS, Beaudet F, Carette S, Décary F, Salusinsky-Sternbach M, Hill RO, Gutkowski A, Harth M, Myhal D. Adult Still's disease: manifestations, disease course, and outcome in 62 patients. Medicine (Baltimore). 1991;70(2):118–36. https://doi.org/10.1097/00005792-199103000-00004.
20. Henter J-I, Horne A, Aricó M, Egeler RM, Filipovich AH, Imashuku S, Ladisch S, McClain K, Webb D, Winiarski J, Janka G, for the Histiocyte Society. HLH-2004: diagnostic and therapeutic guidelines for hemophagocytic lymphohistiocytosis. Pediatr Blood Cancer. 2007;48(2):124–31. https://doi.org/10.1002/pbc.21039.
21. Wang X. Firth logistic regression for rare variant association tests. Front Genet. 2014;5:187.
22. Roy SG, Karunanithi S, Dhull VS, Bal C, Kumar R. ^{18}F-FDG PET/CT aids the diagnosis of adult onset Still's disease in a patient with fever of unknown origin. Rev Esp Med Nucl Imagen Mol. 2014;33(6):392–3. https://doi.org/10.1016/j.remn.2014.03.001.
23. Choe J-Y, Chung DS, Park S-H, Kwon H-H, Kim S-K. Clinical significance of ^{18}F-fluoro-dexoxyglucose positron emission tomography in patients with adult-onset Still's disease: report of two cases and review of literatures. Rheumatol Int. 2010;30(12):1673–6. https://doi.org/10.1007/s00296-009-1137-7.
24. Funauchi M, Ikoma S, Kishimoto K, Shimazu H, Nozaki Y, Sugiyama M, Kinoshita K. A case of adult onset Still's disease showing marked accumulation in the liver and spleen, on positron emission tomography-CT images. Rheumatol Int. 2008;28(10):1061–4. https://doi.org/10.1007/s00296-008-0562-3.
25. Solav SV. FDG PET/CT in evaluation of pyrexia of unknown origin. Clin Nucl Med. 2011;36(8):e81–6. https://doi.org/10.1097/RLU.0b013e31821c99b2.
26. Pak K, Kim S-J, Kim IJ, Kim DU, Kim K, Kim H. Impact of cytokines on diffuse splenic 18F-fluorodeoxyglucose uptake during positron emission tomography/computed tomography. Nucl Med Commun. 2013;34(1):64–70. https://doi.org/10.1097/MNM.0b013e3283595cac.
27. Jia J, Shi H, Liu M, Liu T, Gu J, Wan L, Teng J, Liu H, Cheng X, Ye J, Su Y, Sun Y, Gong W, Yang C, Hu Q. Cytomegalovirus infection may trigger adult-onset Still's disease onset or relapses. Front Immunol. 2019;10:898. https://doi.org/10.3389/fimmu.2019.00898.
28. Wouters JM, van der Veen J, van de Putte LB, de Rooij DJ. Adult onset Still's disease and viral infections. Ann Rheum Dis. 1988;47(9):764–7. https://doi.org/10.1136/ard.47.9.764.
29. Chen D-Y, Chen Y-M, Lan J-L, Tzang B-S, Lin C-C, Hsu T-C. Significant association of past parvovirus B19 infection with cytopenia in both adult-onset Still's disease and systemic lupus erythematosus patients. Clin Chim Acta. 2012;413(9–10):855–60.
30. Kumar A, Aster: Robbins and Cotran pathologic basis of disease, Professional Edition, 9th Ed.
31. Zhou X, Li Y, Wang Q. FDG PET/CT used in identifying adult-onset Still's disease in connective tissue diseases. Clin Rheumatol. 2020;39(9):2735–42. https://doi.org/10.1007/s10067-020-05041-3.
32. Zeng T, Zou YQ, Wu MF, Yang CD. Clinical features and prognosis of adult-onset Still's disease: 61 cases from China. J Rheumatol. 2009;36(5):1026–31. https://doi.org/10.3899/jrheum.080365.

33. Wang J, Wang D, Zhang Q, Duan L, Tian T, Zhang X, Li J, Qiu H. The significance of pre-therapeutic F-18-FDG PET-CT in lymphoma-associated hemophagocytic lymphohistiocytosis when pathological evidence is unavailable. J Cancer Res Clin Oncol. 2016;142(4):859–71. https://doi.org/10.1007/s00432-015-2094-z.
34. Kim J, Yoo SW, Kang S-R, Bom H-S, Song H-C, Min J-J. Clinical implication of F-18 FDG PET/CT in patients with secondary hemophagocytic lymphohistiocytosis. Ann Hematol. 2014;93(4):661–7. https://doi.org/10.1007/s00277-013-1906-y.
35. Zheng Y, Hu G, Liu Y, Ma Y, Dang Y, Li F, Xing H, Wang T, Huo L. The role of (18) F-FDG PET/CT in the management of patients with secondary haemophagocytic lymphohistiocytosis. Clin Radiol. 2016;71(12):1248–54. https://doi.org/10.1016/j.crad.2016.05.011.
36. Bracaglia C, Prencipe G, De Benedetti F. Macrophage activation syndrome: different mechanisms leading to a one clinical syndrome. Pediatr Rheumatol Online J. 2017;15(1):5. https://doi.org/10.1186/s12969-016-0130-4.
37. Bleesing J, Prada A, Siegel DM, Villanueva J, Olson J, Ilowite NT, Brunner HI, Griffin T, Graham TB, Sherry DD, Passo MH, Ramanan AV, Filipovich A, Grom AA. The diagnostic significance of soluble CD163 and soluble interleukin-2 receptor alpha-chain in macrophage activation syndrome and untreated new-onset systemic juvenile idiopathic arthritis. Arthritis Rheum. 2007;56(3):965–71. https://doi.org/10.1002/art.22416.
38. Naymagon L, Tremblay D, Troy K, Mascarenhas J. Soluble interleukin-2 receptor (sIL-2r) level is a limited test for the diagnosis of adult secondary hemophagocytic lymphohistiocytosis. Eur J Haematol. 2020;105(3):255–61. https://doi.org/10.1111/ejh.13433.
39. Hayden A, Lin M, Park S, Pudek M, Schneider M, Jordan MB, Mattman A, Chen LYC. Soluble interleukin-2 receptor is a sensitive diagnostic test in adult HLH. Blood advances. 2017;1(26):2529–34. https://doi.org/10.1182/bloodadvances.2017012310.
40. Ruscitti P, Berardicurti O, Iacono D, Pantano I, Liakouli V, Caso F, Emmi G, Grembiale RD, Cantatore FP, Atzeni F, Perosa F, Scarpa R, Guggino G, Ciccia F, Barile A, Cipriani P, Giacomelli R. Parenchymal lung disease in adult onset Still's disease: an emergent marker of disease severity-characterisation and predictive factors from Gruppo Italiano di Ricerca in Reumatologia Clinica e Sperimentale (GIRRCS) cohort of patients. Arthritis Res Ther. 2020;22(1):151. https://doi.org/10.1186/s13075-020-02245-5.
41. Schulert GS, Yasin S, Carey B, Chalk C, Do T, Schapiro AH, Husami A, Watts A, Brunner HI, Huggins J, et al. Systemic juvenile idiopathic arthritis-associated lung disease: characterization and risk factors. Arthritis Rheumatol. 2019;71(11):1943–54.
42. Saper VE, Chen G, Deutsch GH, Guillerman RP, Birgmeier J, Jagadeesh K, Canna S, Schulert G, Deterding R, Xu J, Leung AN, Bouzoubaa L, Abulaban K, Baszis K, Behrens EM, Birmingham J, Casey A, Cidon M, Cron RQ, de A, de Benedetti F, Ferguson I, Fishman MP, Goodman SI, Graham TB, Grom AA, Haines K, Hazen M, Henderson LA, Ho A, Ibarra M, Inman CJ, Jerath R, Khawaja K, Kingsbury DJ, Klein-Gitelman M, Lai K, Lapidus S, Lin C, Lin J, Liptzin DR, Milojevic D, Mombourquette J, Onel K, Ozen S, Perez M, Phillippi K, Prahalad S, Radhakrishna S, Reinhardt A, Riskalla M, Rosenwasser N, Roth J, Schneider R, Schonenberg-Meinema D, Shenoi S, Smith JA, Sönmez HE, Stoll ML, Towe C, Vargas SO, Vehe RK, Young LR, Yang J, Desai T, Balise R, Lu Y, Tian L, Bejerano G, Davis MM, Khatri P, Mellins ED, Childhood Arthritis and Rheumatology Research Alliance Registry Investigators. Emergent high fatality lung disease in systemic juvenile arthritis. Ann Rheum Dis. 2019;78(12):1722–31. https://doi.org/10.1136/annrheumdis-2019-216040.
43. Nielsen BD, Gormsen LC, Hansen IT, Keller KK, Therkildsen P, Hauge E-M. Three days of high-dose glucocorticoid treatment attenuates large-vessel 18F-FDG uptake in large-vessel giant cell arteritis but with a limited impact on diagnostic accuracy. Eur J Nucl Med Mol Imaging. 2018;45(7):1119–28. https://doi.org/10.1007/s00259-018-4021-4.

Publisher's Note